Archives of Hydro-Engineering and Environmental Mechanics
Vol. 51 (2004), No. 1, pp. 25–40

Model of the Water-Hammer Effect considering a Spring Safety Valve

Marian Niełacny

Poznań University of Technology, Institute of Environmental Engineering,
ul. Piotrowo 5, 60-965 Poznań, Poland, e-mail: marian.nielacny@put.poznan.pl

(Received February 02, 2003; revised July 02, 2003)

Abstract

This paper presents a method for calculating the water-hammer effect in a hydraulic system with a spring safety valve. A model of the valve including its dynamic functioning is presented. The developed model enables simulation testing in order to estimate the influence of construction parameters of the spring activated safety valve on pressure changes and on the velocity of fluid flow along the pipe.

Key words: water-hammer, mathematical model

1. Introduction

The effect of rapid pressure increase in a pipeline, known as water hammer, always takes place in cases of sudden change in fluid velocity. Pipelines and equipment undergo rapid changes in pressure which may considerably damage loaded elements. During the design process of water supply systems it is necessary to analyse all conditions which may cause a water hammer effect. Change in pressure can be caused by:

- a sudden closure (opening) of flow by means of a valve on a water line,
- a sudden electric power switch off to the water pump,
- automatic switch off (switch on) of the water pump.

If the above conditions take place, normal design procedure of hydraulic analysis should be extended by the control analysis of the water hammer effect. This enables pointing out of elements where pressure changes may be dangerous due to insufficient mechanical resistance of pipelines.

2. Characterisation of an Anti Water-Hammer Protection Systems

Protection of water lines against water-hammer effect can be achieved by limiting excessive water pressures to values that pipelines can withstand. This can be achieved by:

- increase in valve shutoff time,
- application of pumps with higher moment of inertia,
- water dump by safety valves,
- application of water-air containers,
- introduction of air or water into areas of under pressure,
- installation of non-return valves with circulation or inlet in the flap.

Giving general guidelines concerning which of the above methods should be applied is not possible. Their effectiveness differs, and depends on specific operating conditions, in some cases a particular method may be appropriate, but in others not. Most commonly used equipment, at pump stations, that limits pressure levels due to water hammer effect are water-air containers or mechanical valves. The author has chosen, and described in this article, the spring safety valves. The main advantages of such valves is their relatively simple construction, small outer dimension and low cost. The valves are installed at pump stations, wells or at any element of the pressure pipeline as long as it is easily accessible for conservation purposes.

Safety valves can be basically divided into two groups:

- valves that open when permissible pressure limits are exceeded,
- valves that open when pressure drops below the permissible limit.

The first group of safety valves is described in this article. The advantage of such valves is their capability of instantaneous flow opening when the limit pressure is exceeded (pre-set level of limit pressure). Analysis of valves belonging to the second group along with mathematical models is described by Grabarczyk, Niełacny, Skiba (1977–1980).

Spring safety valve (Fig. 1), simplified diagram shown in Fig. 2, is connected to the water line by connector 7, fluid flows out through outlet 8. Valve head 6 is pressed to the ball seat by spring 3 by means of a valve stem 5 and plate 4. Spring tension can be regulated by rotating sleeve 1 in valve cover 2. Thus, pressure level at which the valve will open, can be changed.

The valve opens when increased pressure overcomes spring resistance, and in consequence the valve head is raised so that fluid can flow out until pressure drops to the pre-set limit level. This will suppress the effect of water hammer. In the low pressure phase the spring of the valve will shut the outlet. The process of opening and shutting the valve will be repeated until the hammer wave dissipates.

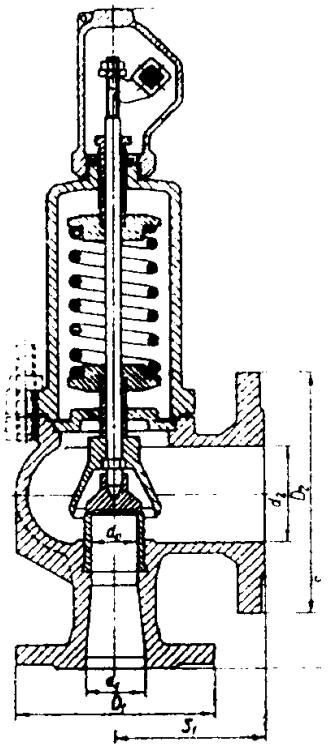

Fig. 1. Spring safety valve

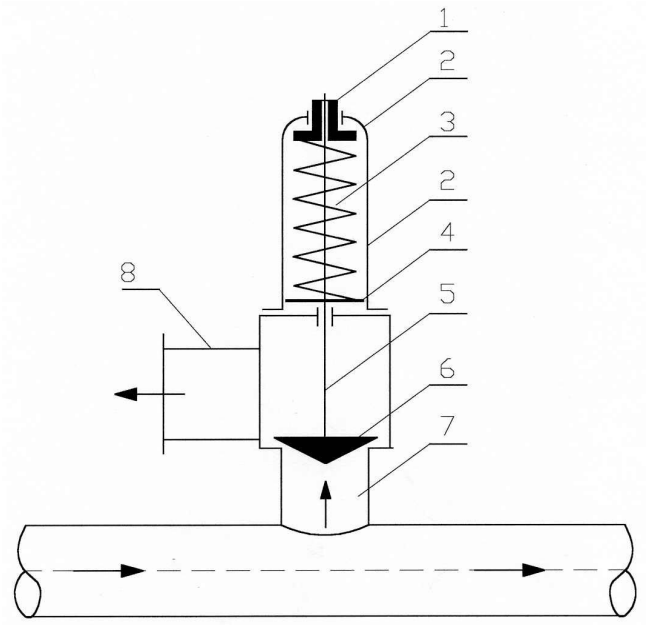

Fig. 2. Simplified diagram of a safety valve

In order to limit the water hammer effect a safety valve should open when pressure rises above a pre-set value, and allow a certain amount of fluid to flow out, so that no further increase in pressure takes place. The value of limit pressure pre-set on the safety valve should be around 10% above operating pressures (Dochnalik 1972, Jankowski 1966). Safety valves, apart from above mentioned advantages, have certain disadvantages such as spring destruction and weakening after a certain period of operation. In this case opening of the valve may not fully eliminate the water hammer effect. Valves should be protected against rust and regularly maintained.

Frequently, data given in literature, concerning different types of valves, describe their construction and operating principles (Dochnalik 1972, Streeter, Wylie 1967, Surin 1967). Sometimes data is given in the form of a diagram showing the effect of water hammer on the system for a particular type of safety valve. In this case the design of valves is limited to determination of the outflow opening diameter based on amount of pressure increase for a system without the valve (Niełacny 1989).

Literature on the water-hammer effect lacks analysis and calculations that take into account the dynamics of valve operation and its behaviour at the moment of the water-hammer effect. This paper presents a mathematical model of a spring activated safety valve including its dynamic action. This enables analysis of combined valve and the hydraulic system by means of computer simulation and allows proper design of dimensions.

3. Principles of Pressure Calculations for Hydraulic Systems with Spring Valves

The hydraulic system which was analysed is shown in Fig. 3.

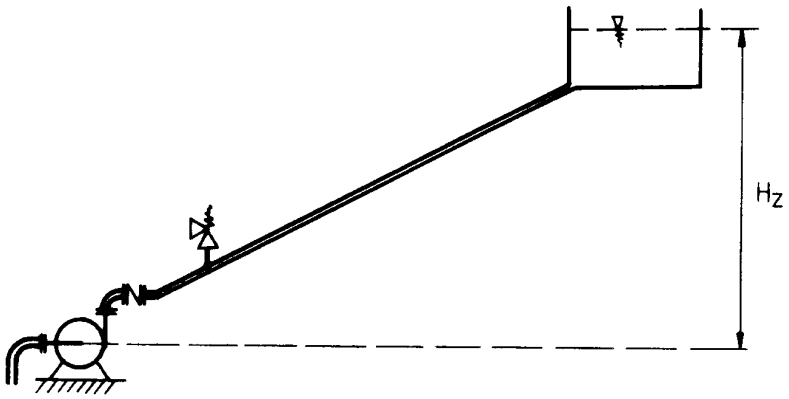

Fig. 3. Simplified diagram of a pump system with a safety valve

Behind the pump a sluice valve is installed. The spring safety valve is placed at the beginning of the pump system. Fluid flows from the pump conduit to a large container.

Mathematical model of the water hammer effect in a closed conduit under pressure is described by a set of two partial differential equations (Fox 1977, Niełacny 1989, Streeter, Wylie 1967).

$$\begin{aligned} &\frac{a^2}{g}\frac{\partial V}{\partial x} + V\frac{\partial H}{\partial x} + \frac{\partial H}{\partial t} + V\sin\alpha = 0, \\ &g\frac{\partial H}{\partial x} + \frac{\partial V}{\partial t} + V\frac{\partial V}{\partial x} + \frac{\lambda\,|V|V}{2D} = 0, \end{aligned} \tag{1}$$

where:

- x – length co-ordinate,
- t – time,
- H – potential head,
- V – flow velocity,
- D – conduit (pipe) diameter,
- g – natural gravity,
- a – increased pressure wave velocity,
- α – inclination angle between conduit (pipe) and horizontal line.

The first is an equation of continuity derived from the law of mass conservation of elastic fluid in an elastic pipe. The second is an equation of momentum conservation that describes dynamic equilibrium of fluid particles in a cross-section of the conduit (pipe). Equations (1) form a closed system of partial differential equations of the hyperbolic type with unknown functions $H(x,t)$ and $V(x,t)$. The system was solved numerically for adequate boundary conditions – according to Fig. 3. In order to solve the system of equations (1) it is necessary to determine pipe pressure wave velocity a and friction factor λ. In works (Evangelisti 1969, Fox 1977, Niełacny 1989, Streeter, Wylie 1967) the calculations of the water-hammer phenomena have been carried out using λ valid for steady-state flow conditions. In this case the description of fluid vibration in a pipe is incorrect as the coefficient λ is much larger for unsteady flow conditions than for steady-state flows. In fact the values of λ for unsteady flows can even be several dozen times greater than these resulting from the Colebrook-White formula.

The characteristics method was used to solve this system of equations (Evangelisti 1969, Niełacny 1987, Niełacny 1989). It enables transformation of the partial differential equations (1) into a system of differential equations, which in turn can be transformed into difference equations, i.e.:

$$
\begin{aligned}
&\frac{\Delta x}{\Delta t} = V + a,\\
&\frac{\Delta V}{\Delta t} + \frac{g}{a}\frac{\Delta H}{\Delta t} + \frac{g}{a} V \sin\alpha + \frac{\lambda |V| V}{2D} = 0,\\
&\frac{\Delta x}{\Delta t} = V - a,\\
&\frac{\Delta V}{\Delta t} - \frac{g}{a}\frac{\Delta H}{\Delta t} - \frac{g}{a} V \sin\alpha + \frac{\lambda |V| V}{2D} = 0.
\end{aligned}
\tag{1a}
$$

Similar derivation is presented by Evangelisti (1969), Niełacny (1989), Streeter, Wylie (1967). Calculations of unknown values of $H(x,t)$, and $V(x,t)$ are performed for a limited number of points (nodes) on the (x,t) plane, called the grid. These points form nodes of the characteristic grid. The calculation process of unknown values of approximate solution of the equation system (1) in individual nodal points of the grid is based on adequate difference equations and for given initial and boundary conditions.

The numerical solution describing the water hammer effect is based on the system of equation (1a). Increments in this system concern changes in time. This means that in order to obtain a solution, valid at a given point in time, parameters known at a previous time point are used. According to the characteristics method, appropriate C^+ and C^- characteristics are inserted into a rectangular grid and then the values of V_P and H_P at grid nodal points P are determined.

The functional diagram shown in Fig. 3 has the following nodes of characteristic grid:

a) internal nodes,
b) boundary node on the side of the pump,
c) boundary node next to the upper equilibrium container,
d) boundary node at safety valve location.

ad. a) Equations for internal nodes.

In order to calculate values of functions $H_P(x,t)$, $V_P(x,t)$ in internal nodes of the grid, finite difference equations are as follows:

$$
\begin{aligned}
V_P = 0.5 \Bigg[& V_R + V_S + (H_R - H_S)\,\frac{g}{a} - \frac{\lambda \Delta t}{2D}\,(V_R\,|V_R| + V_S\,|V_S|) + \\
& - \frac{g}{a}\,\Delta t\,(V_R - V_S)\,\sin\alpha \Bigg],
\end{aligned}
\tag{2}
$$

$$
\begin{aligned}
H_P = 0.5 \Bigg[& H_R + H_S + \frac{g}{a}(V_R - V_S) - \frac{a}{g}\frac{\lambda \Delta t}{2D}\,(V_R|V_R| - V_S|V_S|) + \\
& - \Delta t\,(V_R - V_S)\,\sin\alpha \Bigg],
\end{aligned}
\tag{3}
$$

where:

$$
\begin{aligned}
V_R &= V_O\,[1-\Theta\,(V+a)_O] + V_M\,\Theta\,(V+a)_O,\\
V_S &= V_O\,[1+\Theta\,(V-a)_O] - V_N\,\Theta\,(V-a)_O,\\
H_R &= H_O\,[1-\Theta\,(V+a)_O] + H_M\,\Theta\,(V+a)_O,\\
H_S &= H_O\,[1+\Theta\,(V-a)_O] - H_N\,\Theta\,(V-a)_O,\\
\Theta &= \frac{\Delta t}{\Delta x}.
\end{aligned}
\tag{4}
$$

Indices M, N, O, P, R, S in the above equations relate to nodal points of the grid, and should obtain values interpolated from functions V and H (Fig. 4).

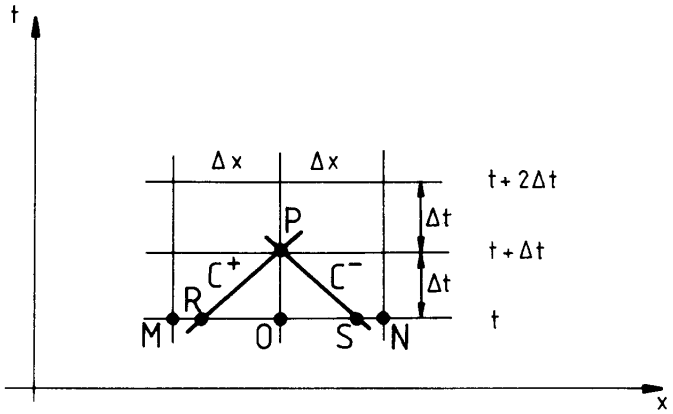

Fig. 4. Basic element of the grid for an internal node

ad. b) Boundary node beside the pump.

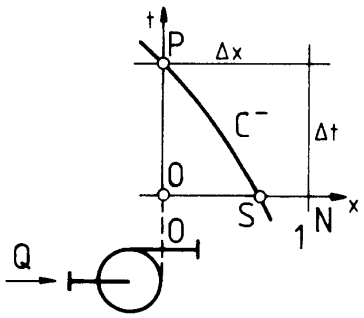

Fig. 5. Grid element of boundary node next to the pump

Calculations of flow velocity V_P and pressure height (head) H_P in the boundary node placed at the beginning of the conduit (Fig. 5) fed by the pump, are performed based on the following equations:

$$V_P = \frac{Q_P}{A}, \tag{5}$$

$$H_P = H_S - V_S \Delta t \sin\alpha + \frac{a}{g}(V_P - V_S) + \lambda \frac{\Delta t}{2D} | V_S | V_S, \tag{6}$$

where $Q_P(t)$ behind the pump, at the end of time interval Δt, is calculated basing on the following equation:

$$Q_P(t + \Delta t) = Q(t) \frac{n(t + \Delta t)}{n(t)}, \tag{7}$$

being similarity law of pump characteristics at rotational velocity change.

Decrease in rotational speed (velocity) of pump units for short time intervals Δt is described by an exponential curve (Fox 1977) in the following form:

$$n(t + \Delta t) = n(t) e^{\frac{Gr}{n} \Delta t}, \tag{8}$$

where:

$n(t + \Delta t)$ – rotational speed of the pump at the end of time interval Δt,
$n(t)$ – rotational speed of the pump at the beginning of time interval t,

$$Gr \cong \frac{dn}{dt} = \frac{3600 N_w}{4\pi^2 I n}, \tag{9}$$

N_w – pump power consumption expressed by the following formula:

$$N_w = \frac{\rho g Q H_u}{\eta}, \tag{10}$$

I – inertia moment of pump rotational elements,
η – pump efficiency,
H_u – useful height of pump elevation.

On the basis of presented equations (7), (8) and characteristic grid, it is possible to determine changes in flow velocities and pressure values behind the pump during stoppage action.

ad. c) Boundary node next to the equilibrium container.

At the boundary node, next to the upper equilibrium container, pressure fluctuation in the conduit does not influence the level of fluid in the container i.e.

$$H(x,t) = H_z = \text{const.}$$

Difference equations in this case have the following form:

$$H_P = H_Z, \tag{11}$$

$$V_P = V_R - \frac{g}{a}(H_P - H_R) - \frac{g}{a}\Delta t V_R \sin\alpha - \frac{\lambda \Delta t}{2D}|V_R|V_R. \tag{12}$$

A diagram for calculations is shown in Fig. 6.

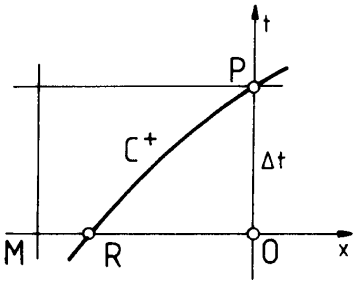

Fig. 6. Basic element of boundary node next to the upper container

ad. d) Boundary node at safety valve location.

A general diagram of connection between safety valve and conduit is shown in Fig. 7.

In order to calculate the magnitude (quantity) of hydrostatic pressure $H_P(x,t)$ and flow velocity $V_P(x,t)$ at boundary point P, situated at the connection of valve and conduit, an equation of a general mathematical model of a valve, given by Grabarczyk, Niełacny, Skiba (1977–1980) was applied. Equations given below are difference equations, describing boundary conditions for a spring safety valve – diagram shown in Fig. 7.

1) Characteristic equation C^+ for j conduit in $N+1$ cross-section

$$\begin{aligned} H_{P_{j,N+1}} = H_R + \frac{a_j}{g}V_R - V_R \Delta t \sin\alpha + \\ - \frac{a_j}{g}\frac{\lambda \Delta t}{2 D_j}|V_R|\, V_R - \frac{a_j}{g}V_{P_{j,N+1}}. \end{aligned} \tag{13}$$

2) Characteristic equation C^- for conduit $j+1$ at cross-section 1

$$\begin{aligned} H_{P_{j+1,1}} = H_S - \frac{a_{j+1}}{g}V_S - V_S \Delta t \sin\alpha + \\ + \frac{a_{j+1}\lambda \Delta t}{2g D_{j+1}}|V_S|\, V_S + \frac{a_{j+1}}{g}V_{P_{j+1,1}}. \end{aligned} \tag{14}$$

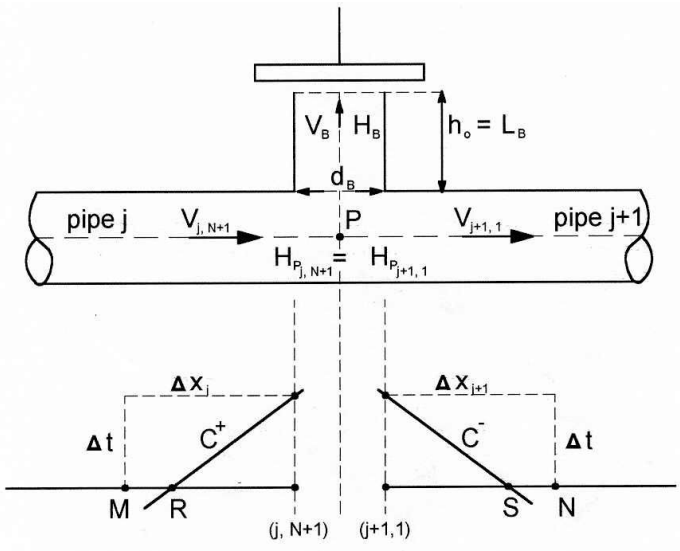

Fig. 7. Basic element for boundary node next to safety valve

3) Pressure compatibility equation at point P, i.e. at valve-pipe connecting point. Conduits (cross-sections) j and $j+1$ are located very close to each other

$$H_{P_{j,N+1}} = H_{P_{j+1,1}}. \tag{15}$$

4) Continuity equation for the T-connection (at valve-pipe connecting point):

$$V_{P_{j,N+1}} A_j = V_B A_B + V_{P_{j+1,1}} A_{j+1} \tag{16}$$

A_j, A_{j+1}, A_B – cross-sectional areas of conduits.

5) Equation of motion for the valve head.
In order to derive the motion equation for the safety valve head, shown in Fig. 8, forces acting on the valve head and pin in the direction of z axis were considered:

– inertia force of the valve head and reduced spring mass:

$$F_b = m\ddot{z}, \tag{17}$$

where:

m – mass of valve parts in motion,
z – height of valve head rise,
$\ddot{z}$ – acceleration along z-axis,

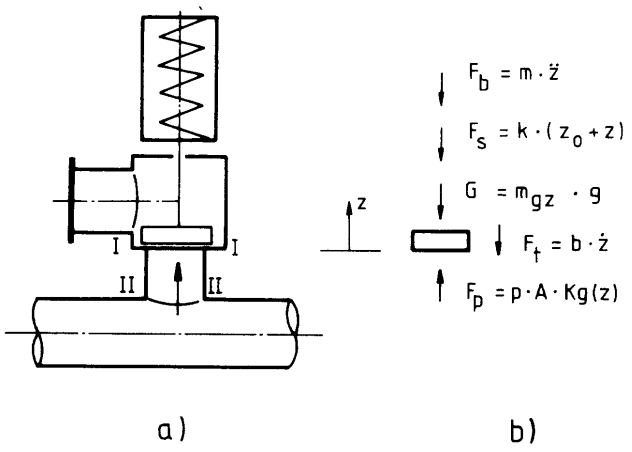

Fig. 8. Basic element for boundary node next to safety valve

– friction force of the pin, holding the valve head:

$$F_t = b\dot{z}, \tag{18}$$

where:

b – index of viscous friction force,
$\dot{z}$ – velocity along z-axis,

– spring force acting on the valve head:

$$F_S = k(z_0 + z) \tag{19}$$

where:

k – spring constant,
z_0 – initial deflection of the spring,

– gravity force of valve head and spring:

$$G = m_{gz}g, \tag{20}$$

where:

m_{gz} – mass of valve head and pin,

– force of hydrodynamic reaction of out-flowing fluid acting on the valve head:

$$F_P = pAKg(z) = \rho g H_B A_B Kg(z), \tag{21}$$

where:

$Kg(z)$ – index of hydrodynamic reaction of fluid on valve head, depends on the degree of valve opening – determined experimentally.

Substituting equations (17)–(21) to the equilibrium equation $\Sigma F = 0$ i.e.:

$$F_b + F_t + F_s + G = F_P, \tag{22}$$

one obtains motion equation for the valve head in the following form:

$$m\ddot{z} + b\,\dot{z} + k\,z + d = pAKg(z), \tag{23}$$

where:

$$d = k\,z_0 + m_{gz}g.$$

6) Motion equation with hydraulic resistance and fluid inertia.
Consider a fluid element limited by planes – I–I in valve head cross-section, and II–II at valve–conduit connection (Fig. 8). The following forces act on the element:

– forces acting on the fluid at the connection from the direction of the conduit:

$$F_1 = \gamma A_B \frac{H_P + H}{2}, \tag{24}$$

where:

A_B – area of cross-section at connecting conduit,
H, H_P – head of pressure at the beginning and end of time interval,

– force acting on the fluid from the direction of the valve:

$$F_2 = \gamma A_B \left(\frac{H_{P_B} + H_B}{2} + L_B \right), \tag{25}$$

where:

L_B – connector length,
H_B, H_{P_B} – pressure height at the beginning and end of time interval, below valve head,

– force related to fluid gravity in the connector:

$$W = \gamma L_B A_B, \tag{26}$$

– friction force in the connector:

$$F_3 = \gamma A_B \left(\frac{\lambda_B L_B}{2g d_B} V_B \mid V_B \mid \right), \tag{27}$$

where:

d_B – connector's diameter,
V_B – fluid velocity in section under valve head.

Making use of Newton's second law, the motion equation of connector, considering the above forces, can be written as follows:

$$\gamma A_B \left[\frac{H_P + H}{2} - \left(\frac{H_{P_B} + H_B}{2} + L_B \right) - L_B - \frac{\lambda_B L_B}{2g d_B} |V_B| V_B \right] = = \frac{\gamma L_B A_B}{g} \frac{dV_B}{dt}. \tag{28}$$

After simplification and approximation of derivative $\frac{dV_B}{dt}$, the following motion equation for the connector is obtained:

$$H_P - H_{P_B} = H_B - H + 4L_B + \frac{\lambda L_B}{d_B g} |V_B| V_B + - \frac{2L_B V_B}{g \Delta t} + \frac{2L_B}{g \Delta t} V_{P_B}. \tag{29}$$

Equation (29) relates pressure in conduit H_P to pressure H_{P_B} under the valve head, depending on fluid flow velocity in the connector.

7) Equation describing flow velocity in the connector under the valve:

$$V_B = \frac{4z\mu(z)}{d_B} \sqrt{2g H_B}, \tag{30}$$

where:

$\mu(z)$ – experimentally determined discharge coefficient of valve, depends on valve opening.

Equations (13), (14), (15), (16), (23), (29), (30) form a closed system of non-linear equations. Solving the system one can determine flow velocity V_P and hydrostatic head H_P at the point of connection between valve and conduit.

4. Initial Conditions

Initial conditions were set for a steady state at time $t_0 = 0$. Thus, known are flow rate and distribution of hydrostatic pressures in all division points at analysed sections.

5. Stability Criteria

In order to assure stability of solution, dimensions of the characteristic grid should be determined according to:

$$\frac{\Delta t}{\Delta x} \leq \frac{1}{|V + a|}. \tag{31}$$

This is the Courant condition (Niełacny 1989, Streeter, Wylie 1967). When this condition is satisfied, characteristics C^+ and C^- intersecting in point P are not beyond interval MN (Fig. 4). This guarantees that deviations at any phase of calculations are transferred with a diminishing amplitude.

6. The Example of Calculation

Pump system with one or two safety valves shown in Fig. 3 is taken into consideration. Pump system data are as follows:

- pipe length $L = 1500$ m
- pipe diameter $D = 1$ m
- initial flow velocity $V = 1$ m/s
- pipe roughness $k = 1.5$ mm
- pump efficiency $\eta = 0.7$
- pump speed $n = 1400$ r/min.

The nominal diameter of the safety-spring-valve (type Si 6301) is $D_{nom} = 150 \times 200$ mm, through outlet diameter is $d_0 = 0.11$ m, spring constant is $k = 504234$ N/m and valve capacity coefficient is $\mu = 0.76$.

It was assumed that the water-hammer is caused by sudden pump disconnection.

In Fig. 9 results of pressure calculation are presented. The values of pressure were obtained for the friction factor $\lambda = 0.0219$ calculated from Colebrook-White formula. The friction factor was determined at the pump outlet cross-section. The results shown in Fig. 9 concern the following pump systems:

- without valve, curve 1
- with one valve, curve 2
- with two valves, curve 3

For the same three pump systems new calculations have been carried out, using the friction factor $\lambda = 0.219$, i.e. 10-times greater than that for steady-state flow conditions. The results of calculations in the form of pressure changes are shown in Fig. 10. The maximum values of pressure are presented in Table 1.

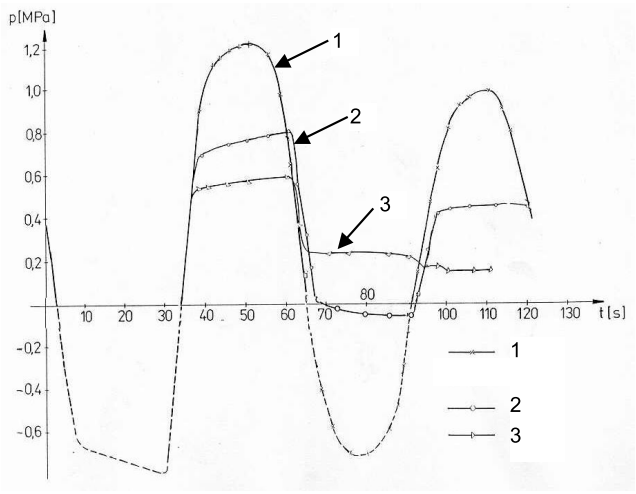

Fig. 9. Changes of pressure behind the pump $\lambda = 0.0219$;
curve 1 – without valve, curve 2 – with one valve, curve 3 – with two valves

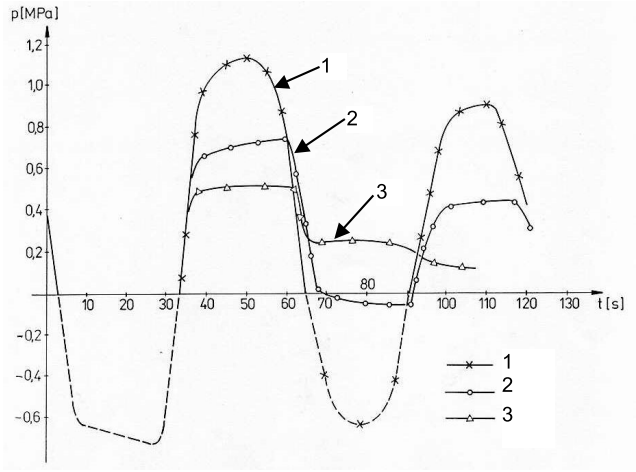

Fig. 10. Changes of pressure behind the pump $\lambda = 0.219$;
curve 1 – without valve, curve 2 – with one valve, curve 3 – with two valves

Table 1. Maximum values of pressure – results of calculations for three pump systems

λ	Maximum values of pressure (results of calculation) p [MPa]		
	without valve	one valve	two valves
0.0219	1.22	0.81	0.59
0.219	1.13	0.74	0.51

As one can see in Figures 9 and 10 and Table 1, for each pump system the maximum values of pressure obtained for friction factor $\lambda = 0.219$ are considerably lower than those for $\lambda = 0.0219$ resulting from the Colebrook-White formula. The pressure changes shown in Figures 9 and 10 confirm that the spring valves can effectively reduce pressure increase resulting from the water hammer phenomenon. The effect of pressure reduction can be simulated using larger values of the friction factor than the values obtained from Colebrook-White formula. The above presented results of calculations, obtained for greater values of the friction factor λ, were not verified experimentally yet. Therefore, it is difficult to determine appropriate (precise) values of the enlargement factor of λ.

7. Final Conclusions

The method of characteristic, presented in this paper, applied to estimate unsteady flow, enables consideration of different boundary conditions and analysis of unsteady states in a hydraulic system which is a part of a water-works system.

The model presented can be applied to a computer programme and to simulation testing in order to estimate the influence of construction parameters of the valve on the water hammer effect. Results of this investigations should be the basis of a rational design procedure for safety valves.

References

Dochnalik K. (1972), TThe Suppressing of Noise in Water Pipes, *Gases, Water and Sanitary Technique*, Part 2, No. 4, 83–88, 122–127 (in Polish).

Evangelisti G. (1969), Waterhamer Analysis by the Method of Characteristics, *L' Energia Elettrica*, No. 10, 11, 12, 673–692, 759–770, 839–858.

Fox J. A. (1977), *Hydraulic Analysis of Unsteady Flow in Pipe Networks*, Mc Press, London.

Grabarczyk Cz., Niełacny M., Skiba J. (1977–1980), *Review of the Methods of Water-Air Reservoirs Design and Construction of Valves, Damping Water Hammer*, Part II, Departmental problem R-15, Poznań–Kraków (in Polish).

Grabarczyk Cz., Niełacny M., Skiba J. (1977–1980a), *Calculation Methodology of Water Hammer Phenomena and Design Principles of Damping Equipment*, Departmental problem R-15, Poznań–Kraków (in Polish).

Jankowski J. (1966), *Pumping Stations and Hydrophore Installation*, Arkady, Warszawa (in Polish).

Niełacny M. (1989), Mathematical modelling of Water Hammer in Irrigational Water Rains Systems, *Monograph Series*, Poznań University of Technology, No. 209 (in Polish).

Niełacny M. (1987), The Method of Characteristics of Solving Quasi-Linear Differential Equations, *Poznań University of Technology Transactions, Series Civil Engineering*, No. 29, 145–157 (in Polish).

Streeter L., Wylie B. (1967), *Hydraulic Transients*, Mc Graw-Hill, New York.

Surin A. A. (1967), *Problems of Water Supply Systems, Water Hammer in Pipelines*, Company Transport, Leningrad (in Russian).